Effect of poly(ether ether ketone) degradation on commingled fabrics consolidation

Feuillerat Lisa, Olivier de Almeida, Fontanier Jean-Charles, Fabrice Schmidt

Effect of poly(ether ether ketone) degradation on commingled fabrics consolidation

Feuillerat Lisa[a,*], De Almeida Olivier[a], Fontanier Jean-Charles[b], Schmidt Fabrice[a]

[a]*Institut Clément Ader (ICA), Université de Toulouse, CNRS UMR 5312, IMT Mines Albi, UPS, INSA, ISAE-SUPAERO, Campus Jarlard, F-81013 Albi, France*
[b]*Institut Français du Textile et de l'Habillement (IFTH), 14 Rue des Reculettes, F-75013 Paris, France*

Abstract

The effects of poly(ether ether ketone) (PEEK) degradation on consolidation of commingled preforms have been investigated. Contrary to what could be expected, under the same processing conditions, consolidation of the preforms systematically results in a high porosity content, above 10%. Fourier Transform Infrared spectrophotometry (FTIR) and Gel Permeation Chromatography (GPC) have shown small molecular structure modifications of PEEK yarns compared to the raw material. These modifications have been attributed to sizing of PEEK filament. Calorimetric (DSC) and rheological analyses have demonstrated that the presence of sizing in the preforms have huge consequences on the degradation kinetics. The crystallization temperature decreases and the viscosity increases significantly. This acceleration of the degradation kinetics is the reason of the poor consolidation behavior during composite manufacturing. The conditions of melt spinning under which the neat PEEK is transformed into filament are therefore a key factor of PEEK degradation.

Keywords: PEEK Degradation, Commingled yarns, A. Preform, E. Consolidation

1. Introduction

Long fiber reinforced thermostable thermoplastic composites have several advantages, such as high thermo-mechanical properties, high chemical resistance and the possibility of

---

*Corresponding author

hot stamping and welding assemblies after consolidation, contrary to thermoset composites [1].

However, the processing of these composites is made complex due to the high melting temperature and high viscosity of thermoplastic matrices. Indeed, at the molten state, high molar mass macromolecules exhibit a non-Newtonian viscosity that is 100 to 1000 times higher than uncured thermosets [2, 3]. Conventional liquid infusion route (RTM or LRI) is no longer possible with polymerized thermoplastic polymers and infusion of reinforcing yarns as described by Darcy's law requires the application of high pressure. The consequence is slow impregnation behavior and non-negligible solid-fluid interaction effects during composites consolidation [2, 4].

In response to this problem, alternative composite products have been developed and various combinations of reinforcements and matrices are now available. The main proposed solutions are pre-impregnated ribbons, commingled yarns, films stacking, powdered yarns or fabrics, or co-woven fabrics [5]. The common point between these different solutions is that the polymer is placed around or within the fiber yarns in order to accelerate the consolidation of the thermoplastic preforms [6, 7]. Even so, high pressure is needed to fully consolidate such semi-finished materials.

Among thermoplastic matrices, semi-crystalline poly-ether-ether-ketone (PEEK) is of particular interest because of its glass transition temperature of 143°C and a service temperature up to 200°C. A temperature of 380 to 400°C is however required to process PEEK composites, and this organic polymer may suffer degradation during each transformation operation.

PEEK degradation above the melting temperature have been many times reported in literature. Day et al. [8–11] have shown that degradation of PEEK results simultaneously in chain cleavage and formation of crosslinks between adjacent aryl groups of polymer chains. The degradation mechanisms have been described in detail by Patel et al. [12]. They showed that PEEK was relatively stable in a non-oxidative environment at 400°C for periods up to 6h, but that the glass transition temperature and the crystallization behavior were rapidly affected under air conditions. Different characterization techniques have been used to describe and confirm PEEK degradation: FTIR and UV-visible spectrophotometry, gel permeation chromatography (GPC), viscosimetry, differential scanning calorimetry

(DSC) and mechanical testing [13–17]. Phillips et al. [18] also confirmed the dominating effect of crosslinking on viscosity and correlated the thermal exposure to air with the compression molding processing behavior of AS4/APC-2 composites. They concluded on the definition of an out-of-autoclave processing limit of carbon/PEEK composites regarding the thermal stability of the matrix.

Even if these studies on PEEK thermal stability propose some guidelines for out-of-autoclave manufacturing of PEEK composites, the authors always assume that the matrix is non-degraded with stable properties before composite processing. This assumption is pertinent when using neat PEEK or pre-impregnated materials made by solvent impregnation (AS4/APC-2 tapes). However, the fabrication of complex semi-finished materials requires several transformation operations that may influence the viscous behavior of the matrix and affect the final processability of the materials. This study therefore aims to determine whether or not the transformation of neat PEEK into a particular architecture has a significant influence on the matrix behavior and the processability of semi-finished composite preforms.

This analysis was conducted by comparing two similar commingled semi-finished products that were manufactured from the same grade of PEEK but supplied by two different suppliers. The processability of the commingled preforms was first evaluated and differences in porosity level were analyzed. A thorough characterization of the PEEK matrices were then performed at the molecular scale using Gel Permeation Chromatography (GPC) and FTIR spectroscopy. Crystallization and viscous behaviors were also studied in order to analyze the properties of the matrix. Differences in consolidation behavior were then analyzed considering the properties of the matrix and a Darcy's law driven impregnation behavior.

2. Experimental

2.1. Materials

Two different carbon/PEEK semi-finished products were investigated. Both are based on the same PEEK grade from Victrex (150). This grade exhibits a glass transition at 143°C and a melting temperature at 343°C as mentioned in the technical data sheet and confirmed by DSC measurements. Both materials were commingled quadriaxial Non

Crimp Fabric (NCF). The NCF weaving structure improves the drapability in comparison with the unidirectional pre-impregnated tape [19].

In order to characterize the microstructure of the materials, pieces of the different semi-finished products were embedded with an ultra-fluid resin, polished and observed with an optical microscope.

The first NCF product (NCF1) has been manufactured by combining together aligned AS4 carbon yarns and PEEK yarns so as to obtain a global commingled structure within each ply. As shown in Figure 1, the commingling level remains poor since no reorganization of PEEK and carbon filaments were performed before the weaving operation. This quadriaxial preform was prepared by stitching together the four commingled unidirectional layers of 145 $\mathrm{g\,m^{-2}}$ each with a PEEK yarn. Two references of the same product were prepared so as to ensure the mirror symmetry: [0/45/90/-45] and [0/-45/90/45].

The second material is also a commingled quadriaxial NCF of AS4/PEEK (NCF2) prepared in the same two stacking configurations [0/45/90/-45] and [0/-45/90/45]. As shown in Figure 2, the commingling level in this material is better than in the NCF1.

These two materials were compared with a 2-faces powdered carbon fabric also based on the same PEEK grade (150). The powdered fabric has a satin weave with an areal weight of 285 $\mathrm{g\,m^{-2}}$. Powdered fabrics are manufactured by heating to melt fine PEEK powder previously sprinkled on a dry fabric. When melted, the polymer droplets coalesce so as to form drops at the surface of the fabrics (Figure 3). When melting, gravity and capillary effects induce a slight migration of the polymer at the surface of the reinforcing yarns. After cooling, the polymer locally rigidifies the resulting semi-finished composite product but the heterogeneous distribution of the drops on the fabric surfaces preserves the global suppleness of the fabric. For this reason, powdered fabrics have a better drapability than the equivalent pre-impregnated products.

2.2. Consolidation of the semi-finished products

Consolidation of carbon/PEEK composites was performed with a thermo-compression molding pilot plant equipped with the 3iTech® technology developed by Roctool. The thermo-compression pilot plant consists of a vertical compression press with a capacity of 1000 kN, a 200 kW induction generator, a cooling unit that can deliver water at a flow rate of 150 $\mathrm{L\,min^{-1}}$ and an inductive mold designed by Roctool. All the equipment are

controlled from an operating panel that centralizes the data (mainly mold temperatures and applied press load) from the different equipment. The 3iTech® mold used in this study is a plane mold designed for composite laminates manufacturing with a molding surface of 400x400 mm². This molding process was used to manufacture 200x200 mm² composite plates of each reference. The thermo-compression cycle applied consisted in a heating phase at $42°C \, min^{-1}$ until 400°C, an isotherm stage at this temperature during 5 to 30 min under a pressure of 9 to 50 bars, and finally in a cooling stage at $20°C \, min^{-1}$.

The Figure 4 shows an example of a thermo-compression cycle applied for the consolidation of a carbon/PEEK semi-finished product. It can be seen that the different monitored parameters perfectly follow the set processing conditions. This control of the processing conditions ensured the repeatability of the consolidation tests.

2.3. Consolidation analysis

Samples cut from the laminates were embedded with an ultra-fluid resin, polished and observed with an optical microscope to assess the consolidation quality. For the optical microscopy tests, a Leica Reichert MEF4 M inverted wide-field microscope with a magnification of 10 times and the bright-field mode was used.

The void ratio (ϕ_{th}) of all composites was then assessed from thickness measurements (th_{plate}) taken at 13 identical locations on the plates after consolidation, compared to theoretical thickness obtained with the initial (A_{ini}) and final (A_{plate}) areas of the plate, the number of layers of semi-finished product (N_{layer}), the fiber (m_{fiber}) and matrix (m_{matrix}) surface densities and the fiber (ρ_{fiber}) and matrix (ρ_{matrix}) densities, using Equation 1.

$$\phi_{th} = 1 - \frac{A_{ini}N_{layer}\left(\frac{m_{fiber}}{\rho_{fiber}} + \frac{m_{matrix}}{\rho_{matrix}}\right)}{A_{plate}th_{plate}} \tag{1}$$

This method to determine the void ratio was compared to the acid digestion technique, achieved following the EN2564 standard. The width, length and thickness of the laminates were 10 mm, 20 mm and about 2 mm respectively. The coupons were weighted (W_{lam}) and the density (ρ_{lam}) was assessed by hydrostatic weighing before dissolution in 30 mL of sulfuric acid at 160°C during 8 h. Then 40 mL of hydrogen peroxide was added drop

by drop. The carbon fibers were filtered, dried and weighed (W_f) to calculate the void ratio (ϕ_{dig}) following the Equation 2, Equation 3 and Equation 4.

$$\phi_{dig} = 100\frac{\rho_{theo} - \rho_{lam}}{\rho_{theo}} \tag{2}$$

with

$$\rho_{theo} = \frac{100}{\frac{1-M_f}{\rho_{matrix}} + \frac{M_f}{\rho_{fiber}}} \tag{3}$$

and

$$M_f = \frac{W_f}{W_{lam}} \tag{4}$$

3. Characterizations of the semi-finished products

In order to analyze the properties of the matrices, the NCF1 and NCF2 PEEK filaments were removed from the different semi-finished products and compared to the Victrex grade 150, provided as a coarse powder (Ref).

The production of micrometer filaments in the spinning process requires a drawing operation which is only possible after applying a sizing on the surface of the extruded yarns. A part of the NCF1 and NCF2 filaments was therefore washed in an ultrasonic acetone bath for 1 h to remove the sizing on the surface of the filaments. This treatment removed most of the sizing from the NCF1 filaments but was not effective for the NCF2 filaments. Only the NCF1-U reference corresponding to unsized NCF1 filaments was therefore analyzed.

3.1. Characterizations of the initial state

Molecular weight distribution of the semi-finished product matrices were determined by Gel Permeation Chromatography (GPC). Measurements were performed by PEAK-EXPERT Company on a Waters 2695 device with a Waters 2414 RID detector. The separation was carried out at 35°C within two Mixed-D Agilent GPC columns from Agilent, with 5 µm particle size, 7.5 mm internal diameter and 50 and 300 mm length, respectively. The eluent was dichloromethane/dichloroacetic acid with 0.01 M of tetrabutylammonium acetate at a flow rate of 1 mL min^{-1}. Samples were prepared by dissolving 20 mg in 10 mL of eluent during 8 h and filtering using filters with 0.45 µm pore size.

FTIR spectra were measured in Attenuated Total Reflection (ATR) mode in the wavelength range from 400 to 4000 cm^{-1} using a Nicolet 6700 instrument from Thermo Scientific. The spectra are the results of 16 recordings with a resolution of 4 cm^{-1}. The results have been normalized by using the absorption band at 1599 cm^{-1} as a reference, which corresponds to elongation of aromatic C=C bond. FTIR spectra (ATR) were also collected on the NCF1 and NCF2 sizing agents. They were obtained after Soxhlet extraction with diethyl ether during 4 h. At the end, the solvent was evaporated to dryness and extracts were weighed in order to estimate the sizing rate.

Matrix filaments were observed under Scanning Electron Microscopy (SEM) using a Hitachi TM3030Plus Tabletop SEM. The diameters of 20 different filaments were measured and averaged to obtain a representative diameter for each composite product.

3.2. Characterizations of the degradation kinetics

Calorimetry measurements were performed with a DSC1 Mettler Toledo. For all experiments, aluminum sealed pans filled with 7 mg $\pm$ 1 mg of PEEK were used. The samples were subjected to 4 heating and cooling cycles in a nitrogen atmosphere, the first one was applied to erase the thermal history. The applied treatment consisted in heating the sample at 20°C min^{-1}, then in holding it at 400°C during 20 min to cause degradation (only 5 min for the first cycle to erase the thermal history), and finally in cooling it at a constant rate of 10°C min^{-1} to induce PEEK crystallization in identical conditions. During this last stage of the thermal treatment, the crystallization temperature (T_c) was measured. T_c has been taken from the maximum of the crystallization peak.

For rheological measurements all the samples (powder and filaments) were prepared with the same method to avoid morphological effects. Filaments were first ground using a Retsch ultra centrifugal mill ZM 100 with a 0.5 mm sieve. The mill was cooled with liquid nitrogen to avoid overheating. Then the powders were compacted with a force of 29 kN during 1 min using an Instron press 5567 and a cylindrical die with a diameter of 20 mm. The obtained tablets were consolidated using a thermo-compression molding pilot process equipped with the 3iTech® technology. The thermo-compression cycle applied consisted in a heating phase at 42°C min^{-1} until 370°C, an isotherm stage at this temperature during 3 min under a force of 125 kN, and finally in a cooling stage at 50°C min^{-1}.

Rheological measurements of PEEK were performed on these consolidated specimens with a Mars Haake rheometer using a plate-plate geometry in oscillatory mode with disposable alumina plates of a diameter of 20 mm. During isothermal experiments, constant shear and shear rates respectively of 0.01 and 6.28 s^{-1} (1 Hz) were applied, at 400°C. In order to guarantee the linear viscoelastic domain, strain sweep tests were previously performed in order to be able to determine the complex viscosity simply from the elastic and viscous moduli G' and G".

4. Results and discussion

4.1. Consolidation analysis

Optical micrographs of composite plates after consolidation presented in Figure 5 show a lot of black areas for the NCF1 and NCF2 compared to the powdered fabric. These black areas correspond to porosities which means that the NCF1 and NCF2 are not well consolidated compared to the powdered fabric. The microstructure of NCF1 reveals that the porosity is located within the carbon yarns. This is the consequence of the low commingling level in NCF1. When melting, the PEEK filaments form a liquid bed surrounding the carbon yarns and composite consolidation is achieved from a radial impregnation process that can be described with Darcy's law [20]. Conversely, the homogeneous distribution of PEEK and carbon filaments in NCF2 leads to porosities both in matrix and carbon-rich areas.

The Figure 6 presents the void ratio of the NCF1, NCF2 and powdered fabric after consolidation, obtained by two methods : thickness measurements and acid digestion. The thickness measurements method seems to over-estimate the void ratio compared to the acid digestion method, but this methods remains a reliable first approach for estimating the void ratio. The NCF1 and NCF2 have a high void ratio after consolidation at 400°C during 10 min under 9 bars, above 10 %, which is not acceptable for high performances composites. This poor consolidation level will result in reduction of the mechanical properties of the final composites [2]. This result confirms the previous optical observations and is quite surprising since polymer flow distance for impregnation is highly reduced in commingled semi-finished products compared to powdered fabrics [20–23].

The Figure 7 shows the effect of pressure and consolidation time on the void ratio of the NCF1 and NCF2 plates. Increasing the consolidation pressure decreases the void ratio, which is in agreement with a Darcy's Law description [2, 24], but all configurations led to a the void ratio above 10 %, even when using pressures up to 50 bars.

Increasing the consolidation time up to 30 min seems to have no effect on void ratio which still remains above 10%. Longer processing times, beyond 30 min, were not explored since degradation may occur. Different temperatures, between 380 and 440°C were also tested but they did not lead to better consolidation level. In addition, a temperature above 400°C is critical for PEEK integrity.

The results of consolidation levels thus demonstrate that an initial optimized semi-finished product architecture is not necessarily optimal for consolidation. In the case of commingled products, the operations necessary for their preparation are obviously responsible for the low level of quality. The spinning of the polymer filaments, which involves an extrusion step at about 400°C and stretching rates of about 100 [25, 26], is one of the factors that can explain the altered processability of semi-finished products. Indeed, at this temperature, degradation can occur [8–11, 13, 15]. Nevertheless, this process also involve drawing above the glass transition temperature and the addition of sizing agents. An analysis of the properties of the matrix has therefore been conducted to identify the origin of this particular behavior.

4.2. Characterization of the initial state

In order to understand possible modifications of PEEK matrix during transformation from neat PEEK to commingled semi-finished products, the different matrix filaments of the NCF1 and NCF2 were characterized and compared to the initial Victrex grade (Ref), provided as a coarse powder.

The molar mass distributions of the NCF1 and NCF2 matrix filaments are compared to the reference in Figure 8. Less than 2% of insoluble were measured for all samples. It can be noticed a slight shift towards lower molar mass for the NCF1 and NCF2 compared to Ref. This is confirmed by the weight average molecular weight (M_w), the number average molecular weight (M_n) and the polydispersity index (IP) presented in Table 1. It can be observed a decrease of M_w (9 % for NCF1 and 11 % for NCF2) as the IP (7 % for

NCF1 and NCF2), but a relatively stable M_n compared to the reference (0.3 % for NCF1 and 3 % for NCF2).

The GPC results therefore show molecular differences between neat (Ref) and transformed PEEK matrices (NCF1 and NCF2). These differences indicate that chain scissions occurred during the extrusion of neat PEEK into the NCF1 and NCF2 filaments. A shift of molar mass distributions towards lower molar mass has indeed already been reported for PET, PLA, PA6 and PP in the case of repeated extrusion [27–30]. Moreover, the NCF1 and NCF2 filament diameters are 25 and 18 µm respectively and as oxygen enhances PEEK degradation [14], the higher surface-to-volume ratio of NCF2 filaments may be a reason of its lower M_n and M_w.

FTIR spectra of the PEEK filaments from the semi-finished products and PEEK reference (Ref) are presented in Figure 9. Between 2800 and 3000 cm^{-1}, two IR absorption bands centered at 2850 and 2935 cm^{-1} appear for the NCF1 and NCF2 that can be attributed to the stretching vibrations of the aliphatic C-H bonds. In the hydroxyl zone between 3200 and 3700 cm^{-1}, a little increase of the large absorption band attributed to stretching vibrations of the O-H bonds of aliphatic groups can also be observed.

Soxhlet extractions were carried out on the NCF1 and NCF2 to separate filaments from the sizing agents. Extracts weighing after Soxhlet extraction have allowed to estimate the sizing rate of 0.45% and 0.27% for the NCF1 and NCF2 respectively. FTIR analysis of these residues show that the NCF1 and NCF2 are covered with sizing agents involving epoxy and polyethylene glycol groups respectively.

The comparison of the NCF1 and NCF2 spectra with those of sizing agents shows that the main differences of FTIR spectra are directly related to the presence of the sizing agent. The two IR absorption bands centered at 2850 and 2935 cm^{-1} have the same profile and a higher absorption level occur in the hydroxyl zone. Because of the predominant effect of sizing on the spectra, the reduction of GPC indicators that are observed for the NCF1 and NCF2 matrices could not be identified using FTIR technique. The presence of sizing agents may have hidden the effect of the molecular modifications and the presence of degradation by-products in small quantity and in the same range of wavelength [13, 14].

The NCF1 and NCF2 have a different molecular state compared to the neat PEEK (Ref) with molar mass distributions shifted towards lower molar mass but also contain different sizing agents at the surface of matrix filaments. Therefore, it is not possible to conclude whether this is the modified molecular structure of extruded PEEK filaments or the nature of the sizing agent that is responsible for the low processability of the semi-finished products during thermo-compression.

4.3. Effect of the initial state on the degradation kinetics

To understand the effect of the initial state on the degradation kinetics during consolidation, DSC and rheometry measurements were carried out on the NCF1 and NCF2 matrix filaments. If a neutral atmosphere slows down the degradation process, its effects can still be observed in a non-oxidative environment. Day et al. [8] have indeed noticed that degradation can occur in a nitrogen atmosphere, which consequences are a decrease of the crystallization temperature, the melting temperature and the enthalpies of crystallization and fusion.

The crystallization temperatures (T_c) as a function of DSC cycles are presented in Figure 10 and Figure 11. It can be seen that the crystallization temperature of neat PEEK (Ref) increases slightly along heat treatment cycles. Several factors can initiate an earlier crystallization, but chain scission during the heat treatment cycles of 20 min at 400°C is the most probable mechanism explaining this T_c evolution. Indeed, this chemical modification is the first mechanism of PEEK degradation.

Conversely, the crystallization temperature of the NCF1 and NCF2 filaments decreases significantly along DSC cycles. This lower ability to crystallize indicates that degradation occurred through crosslinking [31]. The change of T_c is already significant after two cycles for the NCF1 (loss of 10°C), while for the NCF2 the decrease is slower. On the other hand, the NCF1 has a crystallization temperature 2°C lower than the Ref from the first isothermal plateau of 5 min at 400°C unlike the NCF2 which crystallization temperature is 10°C lower. The lower crystallization temperature of the NCF2 indicates that the degradation was initiated before DSC treatment. As the filament diameter of NCF2 is smaller than NCF1, it is likely that more severe conditions where applied to this material in the spinning process, and that chemical modifications occurred during the extrusion operation for this material.

When the sizing agent is removed from the NCF1 filaments (Figure 10), the crystallization temperature remains stable (NCF1-U) which clearly demonstrates the crucial effect of sizing on the thermal stability of PEEK. The significant decrease of T_c for NCF1 indicates that the epoxy-based sizing increases the degradation kinetics of PEEK in the DSC environment, whereas the sizing of NCF2 (PEG) has a low effect on the evolution of the crystallization temperature of PEEK during heat treatments.

The viscosity of PEEK reference at different temperatures representative of processing conditions of semi-finished products is presented in Figure 12. Whatever the temperature, the viscosity curves exhibit a rapid increase of the viscosity level after a relatively stable behavior at the early stage of the experiments. Contrary to the neutral DSC environment, rheometry measurements were achieved in air, which results in a faster chemical degradation process. Likewise the decrease of T_c which is observed for the NCF1 and NCF2, this phenomenon thus corresponds to the crosslinking of polymer chains [16, 18, 32]. The initial viscosity is in accordance with the classical temperature dependence of polymer melt behavior. However, the increase in temperature affects the degradation kinetics by accelerating the increase in PEEK viscosity.

The rheological behavior of the different materials at 400°C is presented in Figure 13. The viscosity of Ref at 400°C increases slowly in the first 10 minutes and then rapidly increases after 25 min. In identical conditions, the viscosity of the NCF1 and NCF2 triples in about 10 and 12 min respectively whereas for the Ref it triples in about 22 min. This more rapid increase in viscosity of the NCF1 and NCF2 matrices therefore clearly appears to be the reason for the difficulty in consolidating the commingled semi-finished-products. With a higher viscosity increases in a shorter period, the NCF1 degrades faster than the NCF2. However, its initial viscosity is lower than the NCF2. This difference in initial viscosity can be attributed to the higher sizing ratio in NCF1, as low molecular weight sizing molecules improve the molecular mobility of the polymer chains through a lubricating effect. When the sizing agents is removed from NCF1, the degradation kinetics is significantly reduced. The crystallization and the viscous behavior of NCF1-U approaches that of Ref, which confirms the major role of sizing on the thermal stability of PEEK and therefore on the consolidation of the semi-finished products. The influence of sizing was already identified by Denault at al. [33] but in the case of carbon fiber sizing.

It is therefore possible that the effect of polymer filament sizing induces an additional effect to that of carbon fiber sizing during the composite consolidation.

The increase of viscosity is directly related to the crosslinking of PEEK molecules, and the temporal evolution of the storage (G_S) and loss (G_L) moduli therefore provides additional information on this process. As explained by Chan et al. [32], the intersection point of G_S and G_L curves can be used as an indicator of the crosslinking rate, as it defines a gel point. The Figure 14 presents an example of the evolution of G_S and G_L over time for the NCF1 and Ref, and the Table 2 summarizes the time of this intersection point for the different materials. The intersection occurs after only 11 min and 16 min for the NCF1 and NCF2 respectively, whereas it appears at 31 min for the neat PEEK (Ref). Regarding those data, it can be stated that after the same exposure time, the NCF1 has a higher crosslinking rate than NCF2 and neat PEEK.

5. Conclusion

The consolidation behavior of two PEEK-based commingled semi-finished products has been compared to a powdered fabric made with the same polymer grade. The results show that an optimized distribution of the polymer within the reinforcement is not necessarily optimal for consolidation. The characterization of the initial state of the matrix in the semi-finished products showed that the extrusion and spinning operations required for the preparation of high performance commingled preforms is responsible for an alteration of matrices integrity. In particular, filament extrusion results in a slight shift of the molecular weight distribution towards lower molecular weights. However, although filament manufacturing may induce changes in PEEK crystallization behavior, the DSC and rheological measurements demonstrate that the sizing at the surface of PEEK filaments is the main critical parameter that affects the processability of the advanced semi-finished products. The sizing induces an acceleration of the PEEK degradation process which consequence is a rapid increase of PEEK viscosity and a progressive decrease of crystallization temperature. This study thus reveals that the selection of sizing agents in the filament extrusion process is of prime importance when designing commingled products. Some results indicate an influence of the sizing rate on PEEK properties, but a thorough analysis of the chemical nature of sizing agents needs to be conducted in

order to better understand the interaction of PEEK with its surrounding environment at the molten state. Moreover, the influence of carbon sizing can also induce an additional effect that should be investigated and taken into account when developing carbon/PEEK products.

6. Acknowledgments

References

[1] L. Ye, Z. R. Chen, M. Lu, M. Hou, De-consolidation and re-consolidation in CF/PPS thermoplastic matrix composites, Composites Part A: Applied Science and Manufacturing 36 (7) (2005) 915–922.

[2] M. Hou, L. Ye, H. J. Leeb, Y. W. Maib, Manufacture of a Carbon-Fabric-Reinforced Polyetherimide (CF / PEI) Composite Material, Composites Science and Technology 58 (1998) 181–190.

[3] G. Sala, D. Cutolo, Heated chamber winding of thermoplastic powder-impregnated composites: Part 1. Technology and basic thermochemical aspects, Composites Part A: Applied Science and Manufacturing 27 (5) (1996) 387–392.

[4] A. K. Kadiyala, J. Bijwe, P. Kalappa, Investigations on influence of nano and micron sized particles of SiC on performance properties of PEEK coatings, Surface and Coatings Technology 334 (2018) 124–133.

[5] C. Steggall-Murphy, P. Simacek, S. G. Advani, S. Yarlagadda, S. Walsh, A model for thermoplastic melt impregnation of fiber bundles during consolidation of powder-impregnated continuous fiber composites, Composites Part A: Applied Science and Manufacturing 41 (1) (2010) 93–100.

[6] A. Miller, C. Wei, A. G. Gibson, Manufacture of polyphenylene sulfide (PPS) matrix composites via the powder impregnation route, Composites Part A: Applied Science and Manufacturing 27A (1996) 49–56.

[7] N. Bernet, V. Michaud, P. E. Bourban, J. A. E. Manson, Commingled yam composites for rapid processing of complex shapes, Composites Part A: Applied Science and Manufacturing 32 (11) (2001) 1613–1626.

[8] M. Day, T. Suprunchuk, J. D. Cooney, D. M. Wiles, Thermal Degradation of Poly(aryl-Ether-Ether-Ketone) (PEEK): A Differential Scanning Calorimetry Study, Journal of Applied Polymer Science 36 (28274) (1988) 1097–1106.

[9] M. Day, J. D. Cooney, D. M. Wiles, The thermal stability of poly(aryl-ether ether-ketone) as assessed by thermogravimetry, Journal of Applied Polymer Science 38 (29850) (1989) 323–337.

[10] M. Day, J. D. Cooney, D. M. Wiles, The thermal degradation of poly(aryl-ether-ether-ketone) (PEEK) as monitored by pyrolysis-GC/MS and TG/MS, Journal of Analytical and Applied Pyrolysis 18 (31856) (1990) 163–173.

[11] M. Day, D. Sally, D. M. Wiles, D. Chemistry, Thermal Degradation of Poly(aryl-Ether-Ether-Ketone) : Experimental Evaluation of Crosslinking Reactions, Journal of Applied Polymer Science 40 (30271) (1990) 1615–1625.

[12] P. Patel, T. R. Hull, R. E. Lyon, S. I. Stoliarov, R. N. Walters, S. Crowley, N. Safronava, Investigation of the thermal decomposition and flammability of PEEK and its carbon and glass-fibre composites, Polymer Degradation and Stability 96 (1) (2011) 12–22.

[13] K. Cole, I. Casella, Fourier transform infra-red spectroscopic study of thermal degradation in poly(ether ether ketone)-carbon composites, Polymer 34 (4) (1993) 740–745.

[14] E. Courvoisier, Y. Bicaba, X. Colin, Multi-scale and multi-technique analysis of the thermal degradation of poly(ether ether ketone), Polymer Degradation and Stability 151 (2018) 65–79.

[15] A. Jonas, R. Legras, Thermal stability and crystallization of poly(aryl ether ether ketone), Polymer 32 (15) (1991) 2691–2706.

[16] V. Mylläri, T. P. Ruoko, J. Vuorinen, H. Lemmetyinen, Characterization of thermally aged polyetheretherketone fibres - Mechanical, thermal, rheological and chemical property changes, Polymer Degradation and Stability 120 (2015) 419–426.

[17] K. L. White, L. Jin, N. Ferrer, M. Wong, T. Bremner, H. J. Sue, Rheological and thermal behaviors of commercial poly(aryletherketone)s, Polymer Engineering and Science 53 (3) (2013) 651–661.

[18] R. Phillips, T. Glauser, J. A. E. Månson, Thermal stability of PEEK/carbon fiber in air and its influence on consolidation, Polymer Composites 18 (4) (1997) 500–508.

[19] B. C. Meyer, C. V. Katsiropoulos, S. G. Pantelakis, Hot forming behavior of non-crimp fabric peek/c thermoplastic composites, Composite Structures 90 (2) (2009) 225–232.

[20] N. Bernet, V. Michaud, P.-E. Bourban, J.-A. E. Manson, An impregnation Model for the Consolidation of Thermoplastic Composites Made from Commingled Yarns, Journal of Composite Materials 33 (1999) 751–772.

[21] B.-D. Choi, O. Diestel, P. Offermann, Commingled CF/PEEK Hybrid Yarns for Use in Textile Reinforced High Performance Rotors, in: 12th International Conference on Composite Materials (ICCM), Paris, 1999, pp. 796–806.

[22] C. V. Katsiropoulos, S. G. Pantelakis, B. C. Meyer, Mechanical behavior of non-crimp fabric PEEK/C thermoplastic composites, Theoretical and Applied Fracture Mechanics 52 (2) (2009) 122–129.

[23] M. D. Wakeman, T. A. Cain, C. D. Rudd, R. Brooks, A. C. Long, Compression moulding of glass and polypropylene composites for optimised macro-and micro-mechanical properties—1 commingled glass and polypropylene, Composites Science and Technology 58 (12) (1998) 1879–1898.

[24] J. Chen, K. Wang, A. Dong, X. Li, X. Fan, Y. Zhao, A comprehensive study on controlling the porosity of CCF300/PEEK composites by optimizing the impregnation parameters, Polymer Composites 39 (10) (2018) 3765–3779.

[25] E. S. Ouellette, J. L. Gilbert, Production and characterization of melt-spun Poly(Ether Ether Ketone) fibers for biomedical applications, Polymer 63 (2015) 10–18.

[26] V. Mylläri, M. Skrifvars, S. Syrjälä, J. Pentti, The Effect of Melt Spinning Process Parameters on the Spinnability of Polyetheretherketone, Journal of Applied Polymer Science 126 (2012) 1564–1571.

[27] M. R. Milana, M. Denaro, L. Arrivabene, A. Maggio, L. Gramiccioni, Gel permeation chromatography (GPC) of repeatedly extruded polyethylene terephthalate (PET), Food Additives and Contaminants 15 (3) (1998) 355–361.

[28] J. Shojaeiarani, D. S. Bajwa, C. Rehovsky, S. G. Bajwa, G. Vahidi, Deterioration in the physico-mechanical and thermal properties of biopolymers due to reprocessing, Polymers 11 (1) (2019) 1–17.

[29] K. H. Lee, S. J. Lim, W. N. Kim, Rheological and thermal properties of polyamide 6 and polyamide 6/glass fiber composite with repeated extrusion, Macromolecular Research 22 (6) (2014) 624–631.

[30] V. A. González-González, G. Neira-Velázquez, J. L. Angulo-Sánchez, Polypropylene chain scissions and molecular weight changes in multiple extrusion *, Polymer Degradation and Stability 60 (1) (1998) 33–42.

[31] Z. Zhang, H. Zeng, Effects of thermal treatment on poly(ether ether ketone), Polymer 34 (17) (1993) 3648–3652.

[32] C.-M. Chan, S. Venkatraman, Crosslinking of poly(arylene ether ketone)s 1. Rheological behavior of the melt and mechanical properties of cured resin, Journal of Applied Polymer Science 32 (7) (1986) 5933–5943.

[33] J. Denault, T. Vu-Khanh, Crystallization and fiber/matrix interaction during the molding of PEEK/carbon composites, Polymer Composites 13 (5) (1992) 361–371.
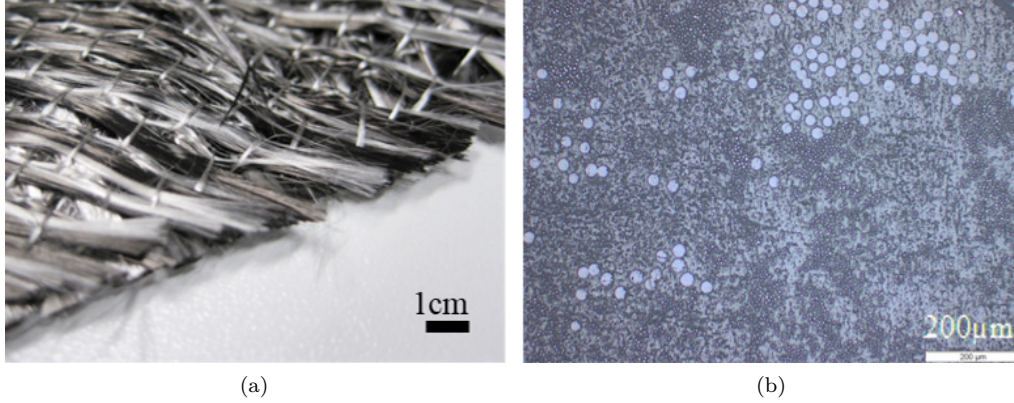
Figure 1: (a) Macroscopic view of the AS4/PEEK NCF1 (b) Cross-section microstructure of a NCF1 unidirectional ply. The white disks with a diameter of about 25 µm are the PEEK filaments and the carbon filaments are the gray small disks (diameter of 7 µm).
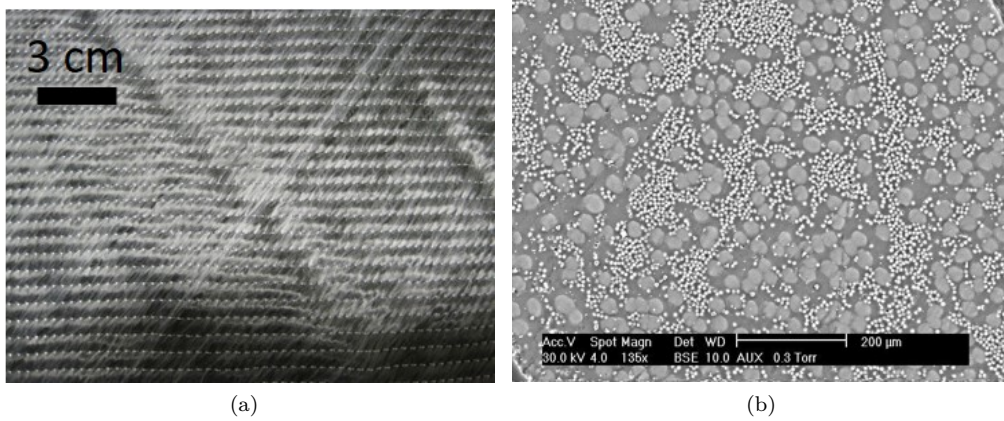

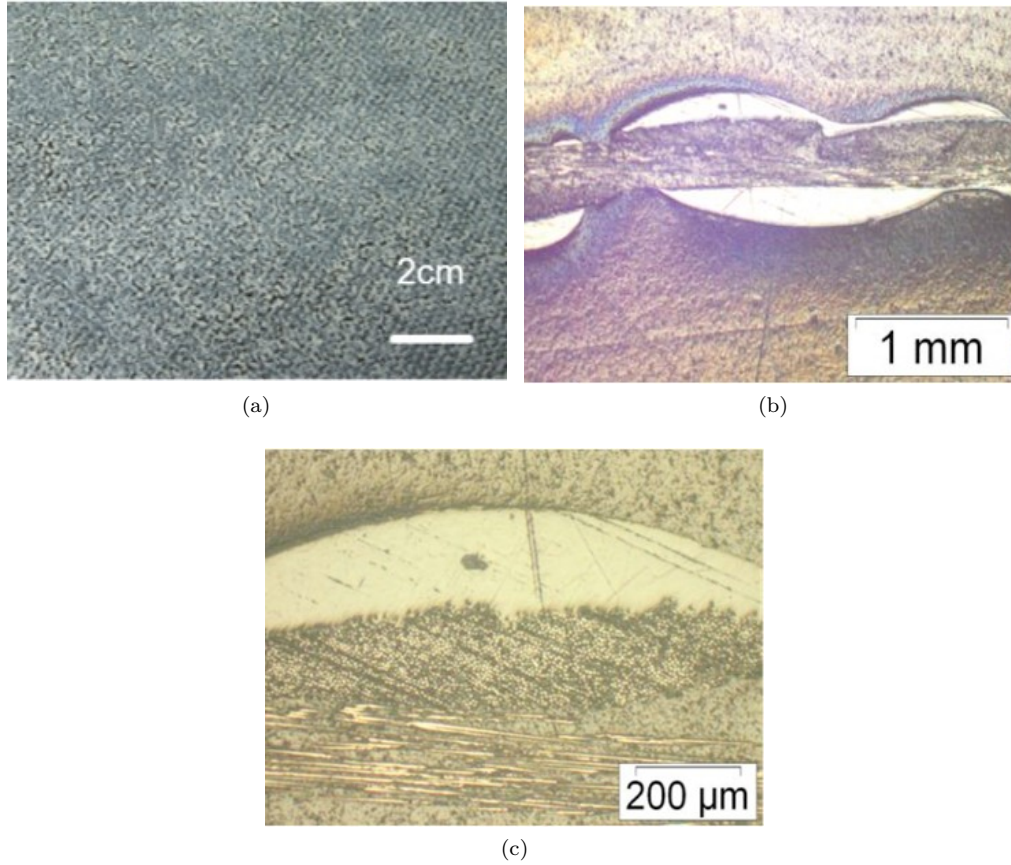Figure 2: (a) Macroscopic view of the AS4/PEEK NCF2 (b) Cross-section microstructure of a commingled yarn in the NCF2. The gray disks with a diameter of about 20 µm are the PEEK filaments and the carbon filaments are the white small disks (diameter of 7 µm).

(a)

(b)

(c)

Figure 3: (a) Macroscopic view (b) Cross-section microstructure x100 (c) Cross-section microstructure x25 of the carbon/PEEK powdered fabric.
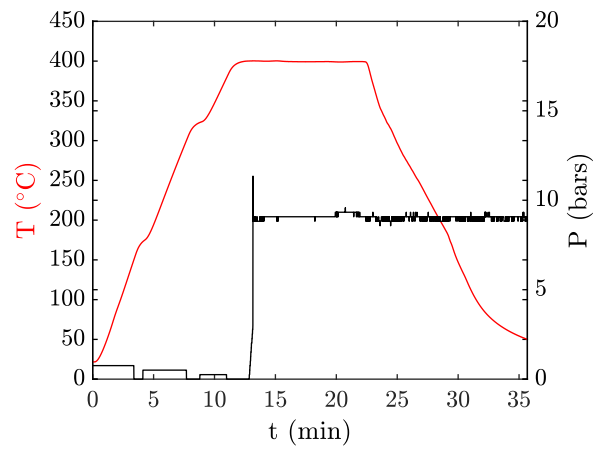
Figure 4: Monitoring of temperature (T) and applied pressure (P) during a thermo-compression cycle of 400°C during 10 min under 9 bars.
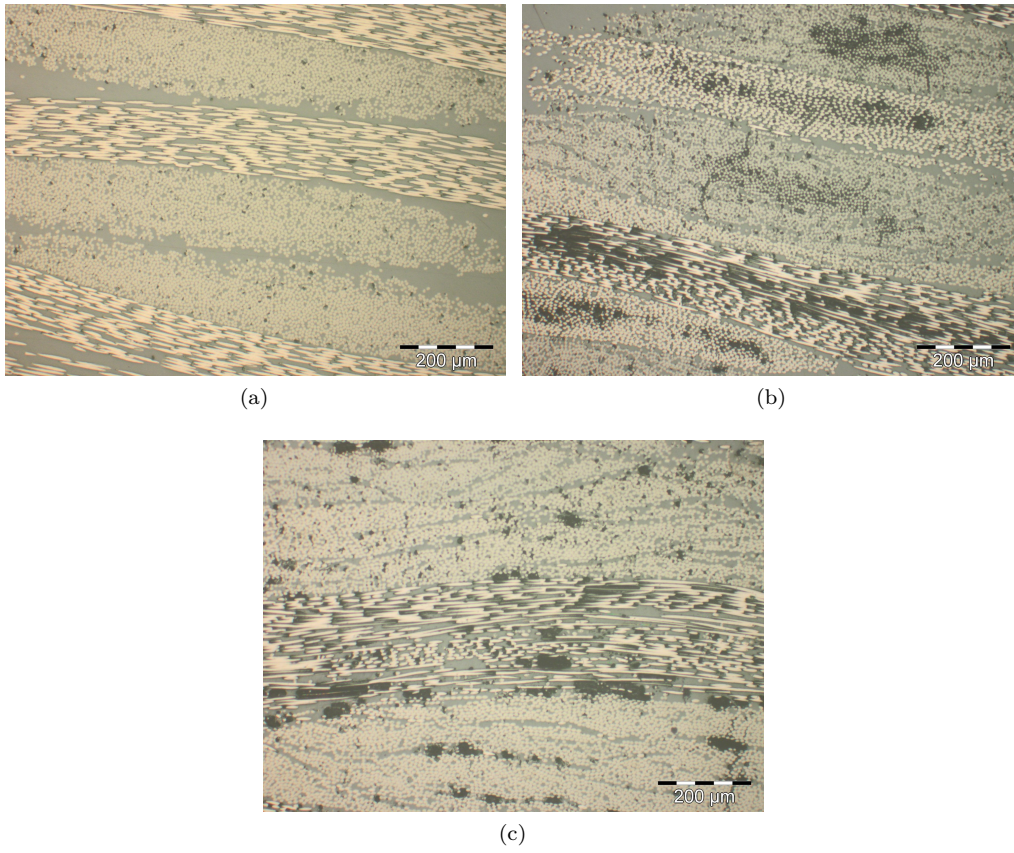
Figure 5: Optical micrographs of the (a) Powdered carbon/PEEK fabric (b) NCF1 (c) NCF2.
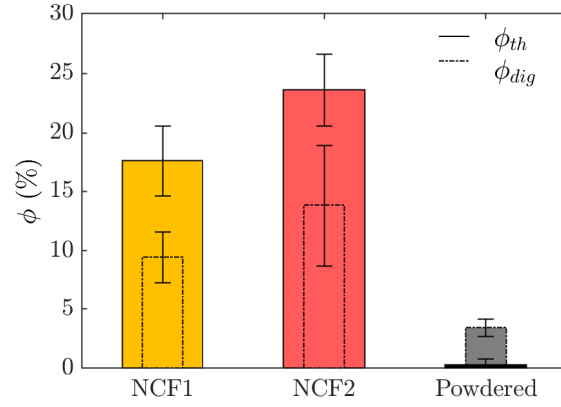
Figure 6: Void ratio (ϕ) of the different semi-finished products after consolidation at $400°C \pm 0.6°C$ during 10 min $\pm$ 0.5 min under 9 bars $\pm$ 0.2 bars, determined from thickness measurements (full line) and acid digestion technique (dotted line).
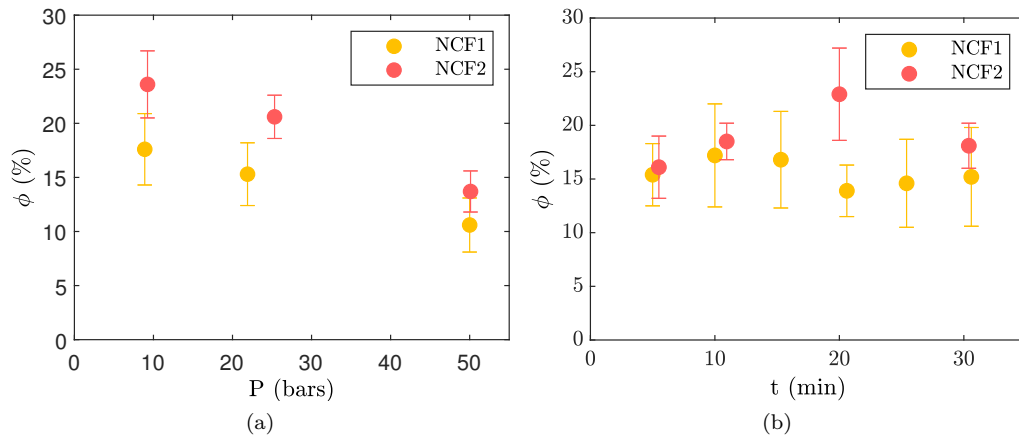
Figure 7: (a) Effect of pressure on void ratio (ϕ) at $400°C \pm 0.4°C$ during 10 min $\pm$ 1 min (b) Effect of time on void ratio (ϕ) at $400°C \pm 0.7°C$ under 25 bars $\pm$ 0.6 bars.
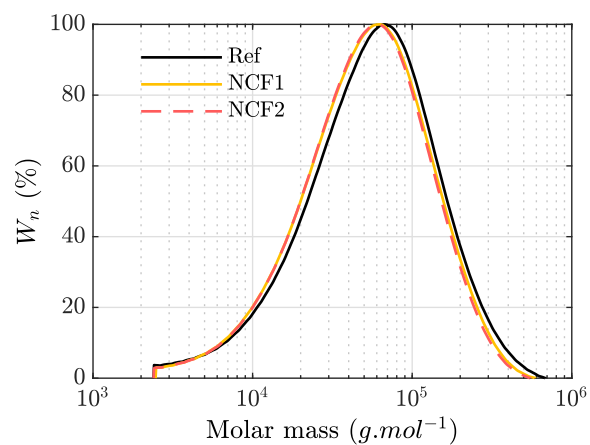
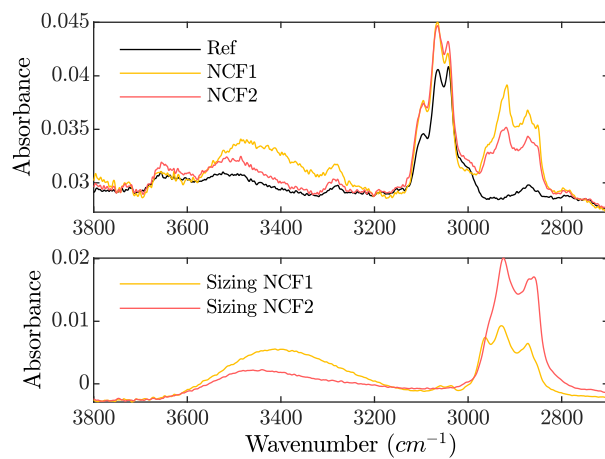Figure 8: Molar mass distributions (normalized weight fraction W_n) of Ref, NCF1 and NCF2.

Figure 9: FTIR spectra : on the top the different semi-finished products (NCF1 and NCF2) and the neat PEEK (Ref), on the bottom the sizing agents of the NCF1 and NCF2.
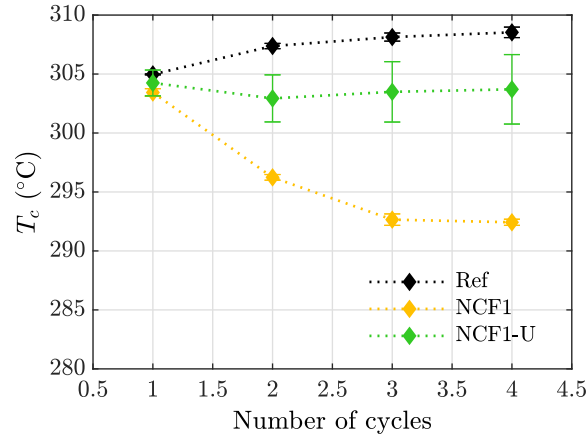
Figure 10: The crystallization temperature T_c (°C) as a function of number of cycles for the NCF1 and the NCF1-U semi-finished products, with and without sizing agents respectively and the neat PEEK (Ref).
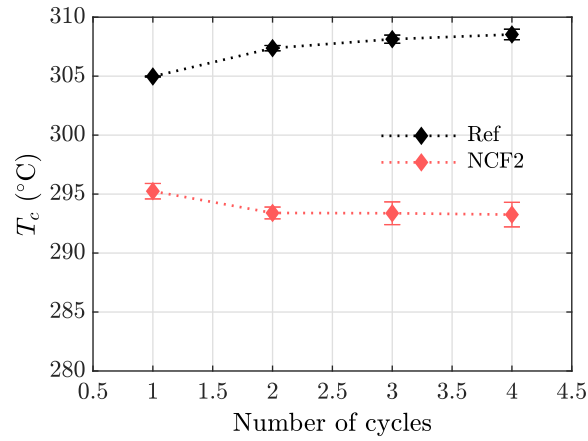

Figure 11: The crystallization temperature T_c (°C) as a function of number of cycles for the NCF2 semi-finished product and the neat PEEK (Ref).
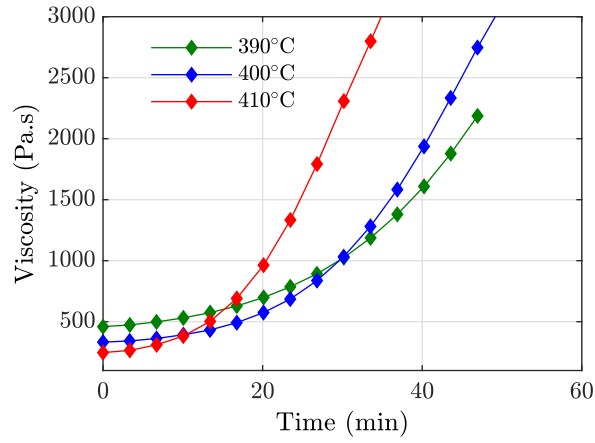
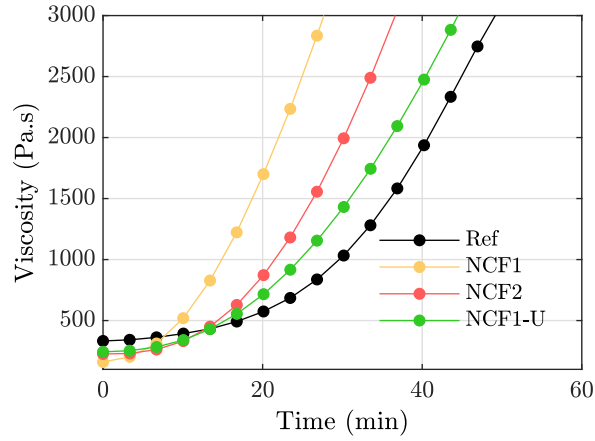Figure 12: Effect of temperature on PEEK viscosity at the molten state.

Figure 13: Time evolution of the viscosity at 400°C for neat PEEK (Ref), PEEK filaments (NCF1 and NCF2), and the NCF1 filaments without sizing agents (NCF1-U).
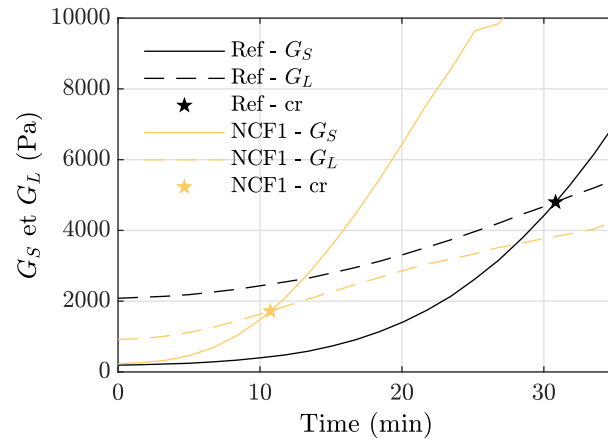
Figure 14: Example of cross-point (stars) between the storage (G_S) and the loss moduli (G_L) at 400°C for the NCF1 and the neat PEEK (Ref).

Table 1: GPC results. Weight average molecular weight (M_w), number average molecular weight (M_n), polydispersity index (IP).

Sample	M_w (g mol^{-1})	M_n (g mol^{-1})	IP
Ref	82097	30291	2.7
NCF1	74273	30198	2.5
NCF2	72433	29392	2.5

Table 2: Time at the cross-point between the storage (G_S) and the loss moduli (G_L).

Sample	Time at the cross-point (min)
Ref	31
NCF1	11
NCF2	16
NCF1-U	21

High viscosity of PEEK

Slow impregnation

Long cycle time

Interest of commingled preforms

Additionnal step in the molten state + addition of sizing

Severe for organic materials Degradation

Carbon reinforcement

PEEK yarns

Commingled preform